Limit Strength of Rectangular Air Ventilation Ducts Under-Seismic Design Condition

T. Kato, T. Nakatogawa
Mitsubishi Atomic Power Industries Inc., Tokyo, Japan
I. Ichihashi
Kansai Electric Power Company, Osaka, Japan
M. Takenaka
Mitsubishi Heavy Industries, Ltd., Takasago, Japan
T. Nomura
Mitsubishi Heavy Industries, Ltd., Kobe, Japan

1. Introduction

The precise estimation of the limiting strength of heating, ventilating, and air conditioning ducts used in nuclear power plants is a key to the safe and economical design of the seismic supports. The formula for estimating the strength of ducts used up to this time, was derived from test results from small size ducts less than 500mm square. This data was extrapolated to obtain the strength of large ducts and therefore big margins had to be used. Consequently the seismic support spans of rectangular ducts are short and a large bulk volume of seismic support material is used in nuclear power plants.

Accordingly, the authors carried out overall pure bending moment tests, shearing load tests, and local buckling load tests using large size rectangular ducts.

In this paper we present the results of these tests and a method of designing seismic supports safely and economically by using the duct limiting strength estimation formula obtained from these tests.

2. Test method

2.1 Bending moment tests

The authors had previously tested square ducts to study the strength of ducts when a pure bending moment was applied about an axis perpendicular to the longitudinal axis of the ducts and the results were reported at the 9th SMiRT conference (Takenaka, 1987).

This time the authors put great emphasis on the effect of the height to width ratio of ducts which will be referred to as the aspect ratio in this paper. One square duct and four rectangular ducts were subjected to four point bending tests as shown in Fig. 1. The dimensions of the ducts is shown in Table-1. The aspect ratio was varied between 1/3 and 3.

An upward load was applied at the ends of each triangular jig until buckling occurred at the corner of the side under compression and the load began to decrease. In these tests the relation between displacements and loads were measured.

2.2 Shearing load tests

Two square ducts were subjected to three point bending load tests as shown in Fig. 2 to study the effect of shearing loads perpendicular to the longitudinal axis of the ducts. The dimensions of the ducts are shown in Table-1. The relation between displacements and loads were measured. The load was applied at the bottom corners of the stiffener which was welded at the center of the duct, until buckling occurred at the corner of the side under compression in the direction of the longitudinal axis of the ducts.

2.3 Local buckling tests

In order to determine the local deformation at the support point, four short square ducts were subjected to three point bending tests as shown in Fig. 3. The dimensions of the ducts are shown in Table-2. The short duct was supported at the stiffener at each end and a support structure which was modeled on the real support structure was attached at the center of the duct. A downward load was applied to the duct through the support structure. The width of the support structure which transmitted the load to the duct was similar to that of a real support.

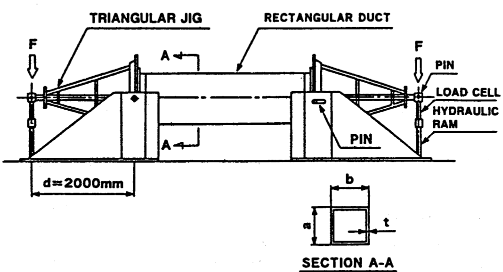

Fig.1 Four Point Bending Test

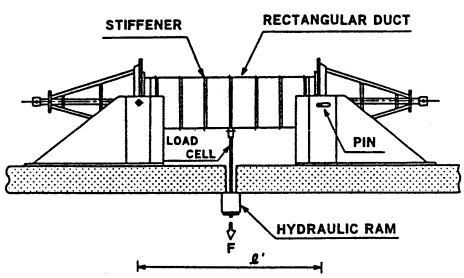

Fig.2 Three Point Bending Test

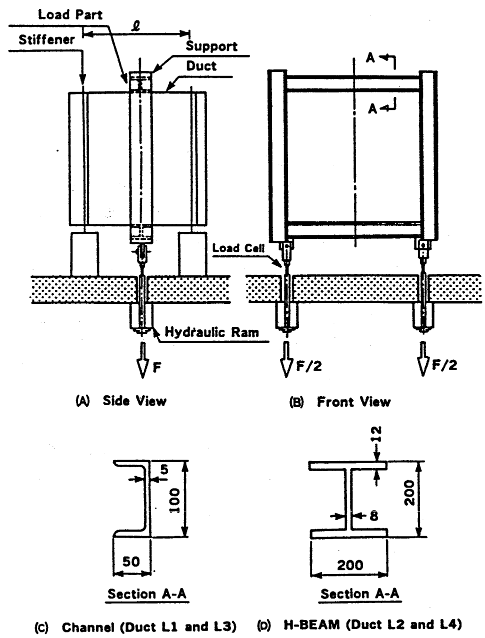

Fig.3 Local Buckling Test at Support Point

3. Test results

3.1 Bending moment tests

The maximum bending moment when buckling occurred at the corner of the side under compression is shown in Table-1.

The longitudinal strain is small in the center part of the compression side flange and is large near the two corners and the other three faces, the other flange and the two webs show the same tendency. The distribution of longitudinal strain differed from that of simple beam theory.

After buckling had occurred on one side, the load was released and an opposite load was applied downwards. The maximum bending moment in this case was almost as large as that when the load was applied upwards.

3.2 Shearing load tests

The maximum bending moment when buckling occurred at the corner of the side under compression is shown in Table-1. The distribution of longitudinal strain showed almost the same tendency as for the bending moment tests.

3.3 Local load tests

The webs near the support points deflected inwards or outwards. The maximum load when buckling occurred in the webs is shown in Table-2.

Table 1 Results of Bending Moment Tests and Shearing Load Tests

Kind of Test	Duct Number	Hight a (mm)	Width b (mm)	Thickness t (mm)	Length ℓ (mm)	a/t	a/b	Modulus of Elasticity E (MPa)	Yield Stress σ_y (MPa)	Measured Moment M^{exp} (N·m)	λ	Predicted Moment M^{pre} (N·m)	$\frac{\sigma^{exp}}{\sigma_y}$	$\frac{\sigma^{pre}}{\sigma_y}$	$\frac{M^{exp}}{M^{pre}}$
Four Point Bending	8	750	750	1.6	2500	469	1	2.02×10^5	307	4.96×10^4	0.996	4.31×10^4	0.135	0.117	1.15
	9	750	375	1.6	2500	469	2	2.02×10^5	307	5.24×10^4	1.05	4.31×10^4	0.142	0.117	1.21
	10	375	750	1.6	2500	234	0.5	2.02×10^5	307	2.77×10^4	1.11	2.16×10^4	0.300	0.234	1.28
	11	1500	500	1.2	4500	1250	3	1.99×10^5	297	6.67×10^4	1.22	4.74×10^4	0.0623	0.0443	1.41
	12	500	1500	1.2	4500	417	0.333	1.99×10^5	297	1.96×10^4	1.07	1.58×10^4	0.165	0.133	1.24
Three Point Bending	13	1500	1500	1.2	6100 (stiffener pitch 1000)	1250	1	2.02×10^5	256	4.42×10^4 (F=38.2kN)	1.06	4.42×10^4	0.0590	0.0480	1.23
	14	1500	1500	1.2	4100 (stiffener pitch 1000)	1250	1	2.02×10^5	256	4.42×10^4 (F=60.0kN)	1.08	4.42×10^4	0.0596	0.0480	1.24

Table 2 Local Load Test Results

Duct Number	Hight a (mm)	Width b (mm)	Thickness t (mm)	Length ℓ (mm)	a/t	a/b	Modulus of Elasticity E (MPa)	Yield Stress σ_y (MPa)	$\frac{a}{t}\sqrt{\frac{\sigma_y}{E}}$	Length of Loading Part N (mm)	Measured Load F^{exp} (N)	Predicted Load F^{pre} (N)	$\frac{F^{exp}}{F^{pre}}$
L1	1500	1500	1.2	1500 (stiffener Pitch 1000)	1250	1	2.02×10^5	256	44.5	50	2.33×10^4	1.70×10^4	1.37
L2	1500	1500	1.2	1500 (stiffener Pitch 1000)	1250	1	2.02×10^5	256	44.5	200	3.01×10^4	2.69×10^4	1.12
L3	750	750	1.6	1400 (stiffener Pitcch 1000)	469	1	2.02×10^5	307	18.3	50	4.36×10^4	2.98×10^4	1.46
L4	1500	1500	3.2	1500 (stiffener Pitch 1000)	469	1	2.10×10^5	278	17.0	200	19.8×10^4	15.9×10^4	1.24

4. Design of seismic supports for ducts

4.1 Seismic support design method for ducts

The design of the locations and styles of duct supports is carried out by applying the maximum allowable seismic support span(MASSS) design technique, following the flow chart shown in Fig. 4. MASSS means the longest span at which ducts can be supported without any damage under seismic conditions. In this technique, ducts are classified into several groups according to buildings, floor elevation, and seismic classification. Then the MASSS of each group is calculated using the single span straight square duct analysis model keeping within the allowable limits for the bending moments and frequencies, etc.

The MASSS values are then multiplied by reduction factors, which are determined by the duct section shapes and the configuration of the duct elements, and are then applied to the whole duct to fix the location of support points in a selected design block. These reduction factors have been derived theoretically or empirically.

4.2 Allowable maximum moment

The allowable maximum moment which is used to calculate the MASSS is derived from the results of bending moment tests as described below.

Applying the effective width theory(von Kārmān, 1932), the maximum bending moment of ducts is given as follows. This has been explained in the previous report(Takenaka, 1987).

$$M = \lambda \sqrt{\frac{E\,\sigma y}{1 - \nu^2}}\, \pi a t^2 \tag{1}$$

where λ, E, σy, ν, a, and t are a constant coefficient, the modulus of elasticity, the yield stress, Poisson's ratio, the duct height, and the thickness respectively.

From the test results, the value of 0.866 is used as a lower bound for λ and the formula (1) becomes:

$$M = 0.866 \sqrt{\frac{E\,\sigma y}{1 - \nu^2}}\, \pi a t^2 \tag{2}$$

A comparison of the test results and the values predicted by formula (2) is shown in Fig. 5. Here the moment is expressed in terms of stress normalized to the yield stress and using the nominal moment of inertia:

$$I = \frac{2}{3} a^3 t \tag{3}$$

Fig. 5 indicates that formula (2) gives a suitable lower limit. After incorporating a suitable safety factor, formula (2) is used as the formula to obtain the allowable moment when calculating the MASSS.

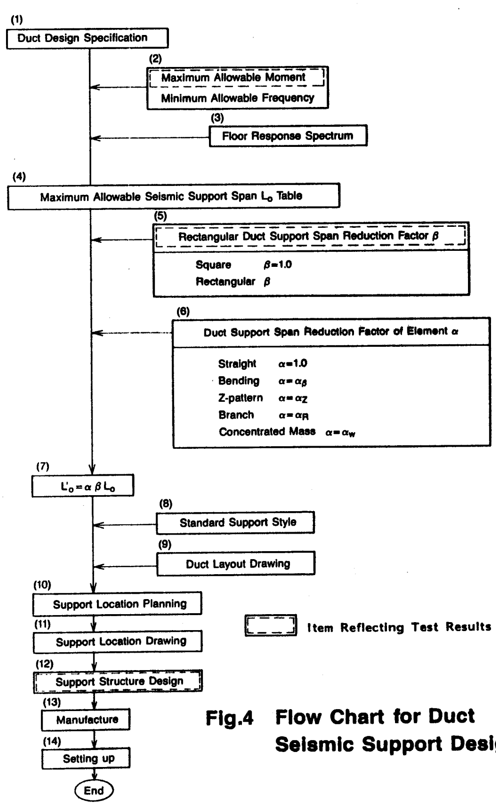

Fig.4 Flow Chart for Duct Seismic Support Design

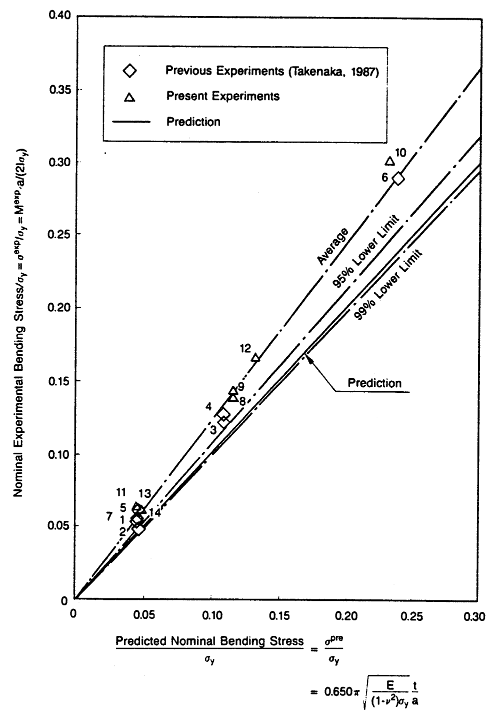

Fig.5 Comparison of Experimental Nominal Bending Stresses with Predicted Values

4.3 MASSS of rectangular ducts

Fig. 6 shows the effect of aspect ratio on the maximum bending moment of the rectangular ducts. This figure indicates that the effect of aspect ratio on the maximum bending moment is very small when the aspect ratios are between 0.33 and 3. From these results, it can be seen that the buckling moment depends on the height, not the width.

The bending moment depends on the support span and weight per unit length. Therefore if the bending moment is to be the same, the support span of a wide duct will be shorter than for a narrow one because its weight per unit length is greater. Considering the weight per unit length of rectangular ducts, the reduction factors for the support spans are derived and applied to the support location design.

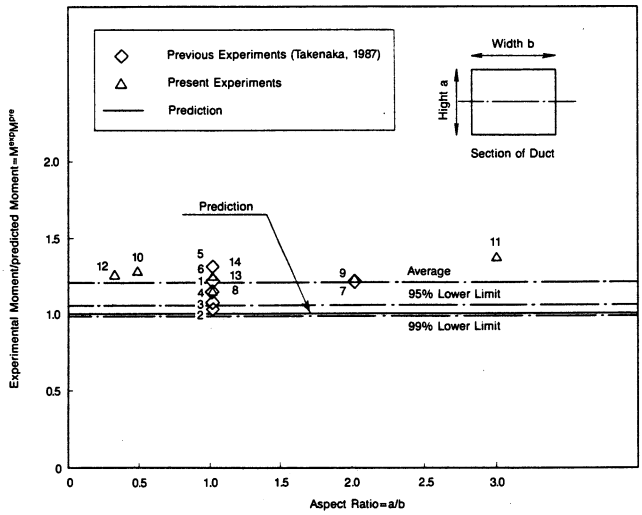

Fig.6 Effect of Aspect Ratio on the Maximum Bending Moment of Rectangular Ducts

4.4 Effect of shearing loads

In spite of the existence of shearing forces, the maximum bending moment in ducts isn't less than the predicted moment calculated by formula (2) as shown in Fig. 5 and Fig. 6. That is the shearing forces have little effect on the maximum bending moment in ducts and they can be ignored in calculating the MASSS as was done for the ducts shown in Table 1.

4.5 The local buckling strength at the support point

As for the local buckling strength at the support points, the authors referred to various sources. The Cold-Formed Steel Design Manual (AISI, 1987) issued by the American Iron and Steel Institute is one of them and gives the formula (Eq. 3.5.1-7) to limit the allowable concentrated loads for cold-formed steel structures. The applicable range of the height to thickness ratio is up to a maximum of 200.

The authors investigated whether this formula can be applied to ducts. The ratio of the measured load to the predicted value is plotted against the plate thickness of the webs in Fig. 7. In this figure, F^{pre}, the predicted maximum buckling local load is evaluated by the following formula. This formula was derived from the AISI's formula (Eq. 3.5.1-7) changing the coefficient.

$$F^{pre} = 3t^2 \sigma y \cdot C_5 C_6 (7.50 + 1.63\sqrt{N'/t}) \qquad (4)$$

where $C_5 = \mathrm{Max}\{(1.49 - 0.53k),\ 0.6\}$

$$C_6 = 0.88 + 0.12m$$
$$k = \sigma y/23.199$$
$$m = t/1.905$$
$$N' = \mathrm{Min}(N, 210t)$$

and t, σy, and N are the thickness of the web, the yield stress, and the length of the webs where the local buckling load is applied. Fig. 7 indicates that formula (4) is a suitable lower limit to predict the maximum concentrated load at the support points of rectangular ducts.

When designing support structures formula (4) is used as the allowable local buckling load taking a safety factor into consideration. If the support load is greater than this allowable load, the width of the support member in contact with the duct at the support point should be increased so as to distribute the load, or the support location should be moved and the support span shortened so as to reduce the support load.

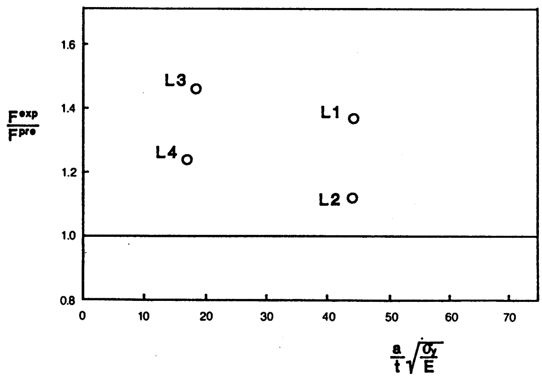

Fig.7 Ratio of Measured Concentrated Load to Predicted Concentrated Load

5. Conclusions

The tests for the limiting strength of rectangular ducts which is necessary for the design of the seismic supports were carried out and the following results were obtained.

(1) For the ducts with the similar sizes and shapes to those which are practically used in the nuclear plants, the formulas estimating more accurately the allowable maximum bending moment and the allowable maximum local buckling load at the support points were obtained.

(2) Shearing forces showed little influence on bending moment, and so they can be ignored in estimating the allowable maximum bending moment.

(3) Design procedure of supports for rectangular ducts was established using these formulas.

The design of seismic support for rectangular ducts can be carried out more safely and economically with these results.

6. Reference

(1) AISI: American Iron and Steel Institute, Cold-Formed Steel Design Manual, 1983.

(2) Takenaka, M., T. Osaki and T. Inoue, Buckling strength of square ducts subjected to bending, Transactions of the 9th International Conference on Structural Mechanics in Reactor Technology, Vol. J, 1987, pp. 29-34.

(3) von Kármán, T., E. E. Sechler and L. H. Donnell, The Strength of thin plates in compression, Trans. ASME, Vol. 54, APM-54-5, 1932, pp. 53-57.